Synthesis and Characterization of Rhenium(III) Complexes with $(Ph_2PCH_2CH_2)_2NR$ Diphosphinoamine Ligands

Received 00th January 20xx,
Accepted 00th January 20xx

DOI: 10.1039/x0xx00000x

Nicola Salvarese,†*[a,b] Fiorenzo Refosco,[a] Roberta Seraglia,[a] Marco Roverso,[a,c] Alessandro Dolmella,[b] Cristina Bolzati†*[a,b]

The synthesis and characterization of a new series of neutral, six-coordinated compounds $[Re^{III}X_3(PNPR)]$, where X is Cl or Br and PNPR is a diphosphinoamine having the general formula $(Ph_2PCH_2CH_2)_2NR$ (R = H, CH_3, CH_2CH_3, $CH_2CH_2CH_3$, $CH_2CH_2CH_2CH_3$ and $CH_2CH_2OCH_3$) are reported. Stable $[Re^{III}X_3(PNPR)]$ complexes were synthesized, in variable yield, starting from precursors where the metal was in different oxidation states (III and V), by ligand-exchange and/or redox-substitution reactions. The compounds were characterized by elemental analysis, proton NMR spectroscopy, cyclic voltammetry, UV/vis spectroscopy, positive-ion electrospray ionization mass spectrometry (ESI(+)-MS) and X-ray diffraction analysis. Although the formulation of the complexes allows either meridional or facial isomers, the latter arrangement was prevalent both in solid and in solution state. Only $[ReCl_3(PNPH)]$ showed a meridional configuration both in solution and in the crystalline state. $[ReBr_3(PNPme)]$ prefers the meridional configuration in the crystalline state and the facial one in solution. While ESI(+)-MS and voltammetric data seems to indicate some dependency from the nature of the alkyl substituent at the nitrogen, the available structural data of the complexes show only slight differences both for angles and bond lengths upon change of the alkyl chain tethered to the nitrogen.

Introduction

Rhenium and technetium represent an attractive pair of metals in the developing of "matched-pair" radiopharmaceutical agents useful in theranostic applications (rhenium-188 for therapy and technetium-99m for Single Photon Emission Computed Tomography, SPECT).[1,2,3]

Despite many efforts, however, the current use of ^{188}Re-based compounds as therapeutical agents is very rare or, at best, at an experimental phase, and it is not predictable whether a ^{188}Re-radiopharmaceuticals will appear on the market.[2] For these reasons, studies aimed to develop new chelating systems, able to provide very stable complexes, and to full understand the ligand coordination properties, remain a valid research focus. Diphosphinoamine (PNP) are an interesting class of ligands which showed excellent coordination properties toward high valent technetium(V) and rhenium(V) species containing metal–nitrogen multiple bonds (terminal nitride[4,5] and phenylimido group[6]). Over the past years, we have dedicated our efforts to thoroughly investigate the reactivity of this kind of ligands toward the nitride-Tc(V) and -rhenium(V) core ($[M^V{\equiv}N]^{2+}$, M = Tc, Re). By using PNPR ligands, it was possible to prepare heteroleptic complexes of the type $[M^V(N)(XY)(PNP)]^{0/+}$, where XY is a bidentate ligand containing soft π-donor/σ-donor coordinating atoms like the couples: NH_2,S^- or S,S^- or O^-,S^-.[4] Remarkably, this chemistry efficiently works also at the tracer level both with technetium-99m[5b,e–j] and rhenium-188.[5k,l] These complexes are characterized by a pseudooctahedral geometry[5a], in which the two phosphorous atoms of the diphosphinoamine are reciprocally *cis* positioned, whereas the amino nitrogen is positioned in *trans* with respect to the M≡N linkages. The nature of the amino group and the length of the alkyl chains between the nitrogen and the phosphorous atoms are crucial factors in determining both the stereochemistry and the reactivity of the intermediate $[M^V(N)Cl_2(PNP)]$ complexes, as well as the stability of the final $[M^V(N)(XY)(PNP)]^{0/+}$ compounds. In particular, when a tertiary amine nitrogen (NR; R = CH_3, $CH_2CH_2OCH_3$) is introduced in the bridging chain, the PNP always adopts a facial configuration, yielding *fac,cis*-$[M^V(N)Cl_2(PNP)]$ compounds as kinetic products.[5b,e] A meridional arrangement of PNPR is instead adopted when the diphosphinoamine incorporates a secondary amine group in the backbone, thus giving the *mer,cis*-$[M^V(N)Cl_2(PNP)]$ species.[5d] It has to be highlightedthat only the *fac,cis*-$[M^V(N)Cl_2(PNP)]$ species promptly undergo ligand exchange reaction, thought the substitution of the electron withdrawing and geometrically prone chlorine atoms with a suitable bidentate ligand, to yield the final heteroleptic complex. On the contrary, the *mer,cis*-$[M^V(N)Cl_2(PNP)]$ complexes, in the same reaction conditions, do not exchange the halides[5d], thus indicating the fundamental role played by the nucleophilicity of the amino group.

[a] *ICMATE-CNR, Corso Stati Uniti, 4, 35127 Padova, Italy. E-mail: cristina.bolzati@cnr.it; E-mail: salvarese-lab@yahoo.it.*
[b] *Dipartimento di Scienze del Farmaco, Università di Padova, Via F. Marzolo 5, 35131 Padova, Italy.*
[c] *Dipartimento di Scienze Chimiche, Università di Padova, Via F. Marzolo 1, 35131 Padova, Italy.*
† Working Address: Dipartimento di Scienze del Farmaco, Università degli Studi di Padova, Via F. Marzolo 5, 35131 Padua, Italy

Electronic Supplementary Information (ESI) available: Synthesis of $(PH_2PCH_2CH_2)_2NR$ diphosphinoamine ligands (PNPme, PNPet, PNPpr, PNPbu). List of polydentate ligands used in substitution reactions with *fac*-$[ReCl_3(PNPet)]$ (**2**) and *mer*-$[ReCl_3(PNPH)]$ (**10**). ESI(+)-MS spectra (range: 600 – 1000 m/z) of $[ReBr_3(PNPR)]$ complexes. MS/MS spectrum of the ion $[Re^V(O)Cl_3(PNPme)+H]^+$ at m/z 764. MS/MS spectrum of the $[ReCl_3(PNP2)+H]^+$ ion at m/z 791. ^{1}H NMR spectra (300 Mhz, $CDCl_3$, 298 K) of **1** – **11**. Selected Bond Lengths (Å) and angles (deg) for the complexes **1** – **4**, **10** and **11**. A full version of the crystallographic experimental work, including a detailed discussion of the treatment of disorder in the X-ray structures. Tightest intermolecular interactions for **1** – **4**, **10**, **11** (discussion and table). See DOI: 10.1039/x0xx00000x. Crystallographic data: CCDC 1532872 (**1**), 1532873 (**2**), 1532874 (**3**), 1532875 (**4**), 1532876 (**10**) and 1532877 (**11**). For crystallographic data in CIF or other electronic format see DOI: 10.1039/x0xx00000x.

Beyond these considerations, indeed the PNP ligands are suitable candidates for the stabilization of rhenium and technetium in lower oxidation states M(I) – M(IV).[7] In particular, complexes with alkylic PNP ligands (i.e. bis[(2-dialkylphosphino)ethyl]amines) were described as useful compounds in catalytic applications.[7g,7l,7n,7o]

Thus, the present study combines our past experience on the $[M^{V}(N)(PNP)]$-complexes with our current interest in the M(III) complexes as potential compounds for radiopharmaceutical applications,[8,9] elucidating the reactivity of a series of diphosphinoamines, showing the general formula $(Ph_2PCH_2CH_2)_2NR$ (here referred as PNPR), toward rhenium(III), and to assess whether the variation of the R substituent at the nitrogen atom affects the coordination geometry and the stability of the complexes as observed for the $[M^{V}(N)(PNP)]$-complexes. The substituents considered are H, CH_3, CH_2CH_3, $CH_2CH_2CH_3$, $CH_2CH_2CH_2CH_3$ and $CH_2CH_2OCH_3$ as sketched in Chart 1.

Starting from the labile oxo-rhenium(V) and rhenium(III) precursor, in this paper we report the syntheses and the full characterization (including the determination of six crystal structures) of a series of neutral rhenium(III) complexes of the type $[ReX_3(PNPR)]$, where X = Cl and Br.

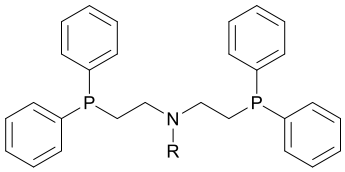

PNPR

R = H	(PNPH)
CH_3	(PNPme)
CH_2CH_3	(PNPet)
$CH_2CH_2CH_3$	(PNPpr)
$CH_2CH_2CH_2CH_3$	(PNPbu)
$CH_2CH_2OCH_3$	(PNP2)

Chart 1 Diphosphinoamines used in our experiments: bis[(2-diphenylphosphino)ethyl]amine (PNPH); bis[(2-diphenylphosphino)ethyl]methylamine (PNPme); bis[(2-diphenylphosphino)ethyl]ethylamine (PNPet); bis[(2-diphenylphosphino)ethyl]propylamine (PNPpr); bis[(2-diphenylphosphino)ethyl]butylamine (PNPbu); Bis[(2-diphenylphosphino)ethyl]methoxyethylamine (PNP2).

Experimental

Materials

All chemicals and reagents were purchased from Aldrich Chemicals (Milano, Italy). The solvents were reagent grade and were used without further purification.

$[NBu_4][ReOCl_4]$, $[ReOCl_3(PPh_3)_2]$, $[ReOBr_3(PPh_3)_2]$ and $[Re^{III}Cl_3(MeCN)(PPh_3)_2]$ were prepared as previously described.[11]

Bis[(2-diphenylphosphino)ethyl]amine hydrochloride (PNPH · HCl) was purchased from Strem Chemicals (Newbury, Ma, USA). Bis[(2-diphenylphosphino)ethyl]methoxyethylamine (PNP2) was prepared by the method published by Morassi and Sacconi[12] and all the other diphosphinoamines by a slightly upgraded procedure as described in ESI.

General note: Due to the tendency of this diphosphinoamine ligands to oxidize, all the operations were carried out under a dinitrogen atmosphere and the solvents used for their preparation or in the complexation reactions were previously degassed.

Physical Measurements

Elemental analyses (C, H, N) were performed on a Carlo Erba 1106 elemental analyzer. ^{1}H NMR spectra of the complexes were acquired at 298 K in $CDCl_3$ on a Bruker AMX 300 instrument, using $SiMe_4$ as internal reference. Common abbreviations for signal multiplicity were used (s = singlet, d = doublets, t = triplets, q = quartets, bs = broad singlet).

Cyclic voltammetry measurements were performed on a BAS (Bioanalytical System Inc.) CV-1B cyclic voltammograph at 293 K under an atmosphere of dinitrogen, in anhydrous deoxygenated dichloromethane solutions (3.5×10^{-3} M) with $[n\text{-}Bu_4N][ClO_4]$ (0.1 M) as the supporting electrolyte, by using a conventional three electrode cell, recording at 0.2 V s^{-1}. A platinum-disk electrode (area ca. 1.28 mm^2) was used as the working electrode, a platinum wire as the counter electrode, and a silver wire as a quasi-reference electrode. Controlled potential coulometries were performed using an Amel model 721 integrator, in an H-shaped cell containing, in arm 1, a platinum gauze working electrode and an Ag/Ag^+ reference electrode isolated inside a salt bridge by a medium-glass frit and, in arm 2, an auxiliary platinum-foil electrode. All potentials were internally referred against the ferrocene couple (400 mV vs NHE).

UV/vis spectra were registered in dichlorometane with a Cary 5E UV/vis spectrophotometer, and normalized at 350 nm (compounds **1**, **2**, **4**, **6**, **8**) or 400 nm (compounds **3**, **5**, **7**, **9**, **10** and **11**).

Mass spectra were obtained using a LCQ Fleet Thermo-Scientific ion trap mass spectrometer equipped with an heated electrospray ionization ion source, operating in positive ion mode. The complexes were dissolved in dichloromethane giving 10^{-2} M stock solutions, which in turn were diluted with acetonitrile to obtain 10^{-5} M final solutions. Experiments were performed by direct infusion of the sample solution via a syringe pump at a flow rate of 13 μL/min. The ions were produced using a spray voltage of 3 kV and entrance capillary temperature of 280 °C in positive ion mode. Other instrumental parameters were automatically adjusted to optimize the signal-to-noise ratio.

Synthesis of the $[ReX_3(PNPR)]$ Complexes

General procedure for *fac*-$[ReCl_3(PNPR)]$ (PNPR = PNPme, PNPet, PNPpr, PNPbu, PNP2). Chloro-complexes were prepared using two different procedures, starting from the rhenium(V) precursors $[Re^{v}OCl_3(PPh_3)_2]$ or $[NBu_4][Re^{v}OCl_4]$, and the rhenium(III) precursor $[Re^{III}Cl_3(PPh_3)_2(MeCN)]$, as described below. Final yields were comparable. *i)* In a two-neck flask containing a suspension of $[Re^{v}OCl_3(PPh_3)_2]$ (153 mg, 0.18 mmol), or alternatively $[NBu_4][Re^{v}OCl_4]$ (0.18 mmol), in ethanol (15 mL), a solution of PNPR (0.27 mmol) in ethanol (5 mL) was added. After the mixture was refluxed for 20 h, an orange precipitate was formed. After cooling, the solid was filtered off and washed with ethanol (3x1 mL) and diethyl ether (2x2 mL).

ii) In a two-neck flask containing the orange suspension of $[Re^{III}Cl_3(PPh_3)_2(MeCN)]$ (100 mg, 0.116 mmol) in ethanol (10 mL), a solution of PNPR (0.116 mmol) in ethanol (5 mL) was added. The reaction mixture was refluxed for 6 hours, and during this time it became clear, while the color turned from orange to orange-brown. After cooling, the brown-orange precipitate was collected by filtration, washed with ethanol (3 mL) and diethyl ether (3 mL), and dried in vacuum.

General procedure for *fac*-[$ReBr_3$(PNPR)] (PNPR = PNPet, PNPpr, PNPbu, PNP2). Bromo-complexes were prepared following the procedure *i* described for *fac*-[$ReCl_3$(PNPR)], by using the precursor $[Re^{V}OBr_3(PPh_3)_2]$ (174 mg, 0.18 mmol).

***fac*-[$ReCl_3$(PNPme)] (1).** Yield 50%. Elem. Anal. Found: C, 46.9%; H, 4.5%; N, 1.7%. Calc. for $C_{29}H_{31}NP_2Cl_3Re$: C, 46.6%; H, 4.2%; N, 1.9%. ESI(+)-MS: *m/z* 748.17 ($[ReCl_3(PNPme)+H]^+$, 100%), 712.26 ($[ReCl_3(PNPme)+H–HCl]^+$, 86%), 676.33 ($[ReCl_3(PNPme)+H–2HCl]^+$, 32%). Other signals in the spectrum are tentatively assigned to oxo-rhenium(V) species: 764.26 ($[ReOCl_3(PNPme)+H]^+$, 93%), 728.23 ($[ReOCl_3(PNPme)+H–HCl]^+$, 18%), 692.43 ($[ReOCl_3(PNPme)+H–2HCl]^+$, 6%).

***fac*-[$ReCl_3$(PNPet)] (2).** Yield 45%. Elem. Anal. Found C, 47.4%; H, 4.5%; N, 1.8%. Calc. for $C_{30}H_{33}NP_2Cl_3Re$: C, 47.3%; H, 4.4%; N, 1.9%. ESI(+)-MS: *m/z* 762.45 ($[ReCl_3(PNPet)+H]^+$, 100%), 726.37 ($[ReCl_3(PNPet)+H–HCl]^+$, 24%), 690.47 ($[ReCl_3(PNPet)+H–2HCl]^+$, 16%). Other signals in the spectrum are tentatively assigned to oxo-rhenium(V): 778.35 ($[ReOCl_3(PNPet)+H]^+$, 9%), 742.42 ($[ReOCl_3(PNPet)+H–HCl]^+$, 4%).

***fac*-[$ReBr_3$(PNPet)] (3).** Yield 14%. Elem. Anal. Found: C, 40.5%; H, 3.5%; N, 1.4%. Calc. for $C_{30}H_{33}NP_2Br_3Re$: C, 40.25%; H, 3.7%; N, 1.6%. ESI(+)-MS: *m/z* 918.00 ($[ReBr_3(PNPet)+Na]^+$, 8%), 895.19 ($[ReBr_3(PNPet)+H]^+$, 100%), 816.15 ($[ReBr_3(PNPet)+H–HBr]^+$, 11%), 734.32 ($[ReBr_3(PNPet)+H–2HBr]^+$, 10%).

***fac*-[$ReCl_3$(PNPpr)] (4).** Yield 47%. Elem. Anal. Found: C, 48.2%; H, 4.6%; N, 1.7%. Calc. for $C_{31}H_{35}NP_2Cl_3Re$: C, 48.0%; H, 4.55%; N, 1.8%. ESI(+)-MS: *m/z* 776.55 ($[ReCl_3(PNPpr)+H]^+$, 89%), 740.46 ($[ReCl_3(PNPpr)+H–HCl]^+$, 100%), 704.56 ($[ReCl_3(PNPpr)+H–2HCl]^+$, 45%). Another signal in the spectrum is tentatively assigned to an oxo-rhenium(V) species: 756.50 ($[ReOCl_3(PNPpr)+H–HCl]^+$, 7%).

***fac*-[$ReBr_3$(PNPpr)] (5).** Yield 11%. Elem. Anal. Found: C, 40.9%; H, 3.8%; N, 1.5%. Calc. for $C_{31}H_{35}NP_2Br_3Re$: C, 41.0%; H, 3.9%; N, 1.55%. ESI(+)-MS: *m/z* 932.03 ($[ReBr_3(PNPpr)+Na]^+$, 13%), 909.20 ($[ReBr_3(PNPpr)+H]^+$, 75%), 830.15 ($[ReBr_3(PNPpr)+H–HBr]^+$, 36%), 748.41 ($[ReBr_3(PNPpr)+H–2HBr]^+$, 55%), 702.49 (100%).

***fac*-[$ReCl_3$(PNPbu)] (6).** Yield 23%. Elem. Anal. Found: C, 48.8%; H, 4.8%; N, 1.7%. Calc. for $C_{32}H_{37}NP_2Cl_3Re$: C, 48.6%; H, 4.7%; N, 1.8%. ESI(+)-MS: *m/z* 790.50 ($[ReCl_3(PNPbu)+H]^+$, 100%) 754.35 ($[ReCl_3(PNPbu)+H–HCl]^+$, 10%), 718.46 ($[ReCl_3(PNPbu)+H–2HCl]^+$, 4%).

***fac*-[$ReBr_3$(PNPbu)] (7).** Yield 9%. Elem. Anal. Found: C, 41.5%; H, 3.8%; N, 1.4%. Calc. for $C_{32}H_{37}NP_2Br_3Re$: C, 41.7%; H, 4.05%; N, 1.5%.

fac-[$ReCl_3$(PNP2)] (8). Yield 35%. Elem. Anal. Found: C, 47.4%; H, 4.6%; N, 1.8%. Calc. for $C_{31}H_{35}NOP_2Cl_3Re$: C, 47.2%; H, 4.5%; N, 1.8%. ESI(+)-MS: *m/z* 792.32 ($[ReCl_3(PNP2)+H]^+$, 100%), 756.31 ($[ReCl_3(PNP2)+H–HCl]^+$, 70%). Another signal in the spectrum is tentatively assigned to an oxo-rhenium(V): 772.29 ($[ReOCl_3(PNP2)+H–HCl]^+$, 8%).

fac-[$ReBr_3$(PNP2)] (9). Yield 12%. Elem. Anal. Found: C, 40.1%; H, 3.5%; N, 1.4%. Calc. for $C_{31}H_{35}NOP_2Br_3Re$: C, 40.3%; H, 3.8%; N, 1.5%. ESI(+)-MS: *m/z* 947.97 ($[ReBr_3(PNP2)+Na]^+$, 19%), 925.16 ($[ReBr_3(PNP2)+H]^+$, 100%), 846.21 ($[ReBr_3(PNP2)+H–HBr]^+$, 76%), 764.28 ($[ReBr_3(PNP2)+H–2HBr]^+$, 3%), 718.40 (83%).

Procedure for *mer*-[$ReCl_3$(PNPH)] (10). In a two-neck flask containing the orange dispersion of $[Re^{III}Cl_3(PPh_3)_2(MeCN)]$ (100 mg, 0.116 mmol) in degassed ethanol (10 mL), solid PNPH · HCl (55.7 mg, 0.116 mmol) was added. To the resulting mixture, triethylamine (0.017 mL, 0.116 mmol) was added under stirring. The flask was refluxed 6 hours during which the color of the mixture turned from yellow to green and a brown precipitate formed. After filtration and washing with ethanol (3 mL) and diethyl ether (3 mL) the solid was dried in vacuum. By dissolving the powder in dichloromethane, brown crystals formed after few minutes. Yield 89%. Elem. Anal. Found: C, 45.9%; H, 4.1%; N, 1.8%. Calc. for $C_{28}H_{29}NP_2Cl_3Re$: C, 45.8%; H, 4.0%; N, 1.9%. ESI(+)-MS: *m/z* 698.62 ($[ReCl_3(PNPH)+H–HCl]^+$, 100%), 662.47 ($[ReCl_3(PNPH)+H–2HCl]^+$, 58%). Another signal in the spectrum is tentatively assigned to an oxo-rhenium(V) species: 678.50 ($[ReOCl_3(PNPH)+H–2HCl]^+$, 10%).

Procedure for [$ReBr_3$(PNPme)] (11). The complex was prepared according to the general procedure for *fac*-[$ReBr_3$(PNPR)] described above. Yield 39%. Elem. Anal. Found: C, 39.7%; H, 3.5%; N, 1.5%. Calc. for $C_{29}H_{31}NP_2Br_3Re$: C, 39.6%; H, 3.55%; N, 1.6%. ESI(+)-MS: *m/z* 881.16 ($[ReBr_3(PNPme)+Na]^+$, 35%), 802.10 ($[ReBr_3(PNPme)+H–HBr]^+$, 73%), 720.41 ($[ReBr_3(PNPme)+H–2HBr]^+$, 100%).

All the complexes are soluble in dichloromethane and chloroform, slightly soluble in acetone and not soluble in acetonitrile, ethanol and methanol.

All complexes are paramagnetic. Nevertheless, ^{1}H NMR data were collected (see ESI, Tables S1 and S2 and Figures S5 – S15).

X-ray Crystallography

X-ray quality crystals of **2** – **4** and **11** were obtained by slow diffusion of methanol in a dichloromethane solution; samples of **1** and **10** were recrystallized from dimethylformamide and dichloromethane, respectively. Data collection were performed at room temperature (294 to 302 K) on an Oxford Diffraction Gemini EOS CCD diffractometer by means of the ω–scans technique, using graphite–monochromated radiation, 1024 × 1024 pixel mode and 2 × 2 pixel binning. Diffraction intensities were corrected for Lorentz and polarization effects; an empirical multi–scan absorption correction, based on equivalent reflections, was applied with the scaling algorithm SCALE3 ABSPACK. Two reference frames were collected after every 50 frames to check for crystal and instrument stability; no change in peak positions/intensities was noticed. Data collection, reduction and refinement were carried out by means of the CrysAlis Pro software suite.[13]

Accurate unit cell parameters were determined by least–squares refinement of highest intensity reflections chosen from the whole experiment. The structures were solved through

direct methods (complexes **1** – **4**) or heavy–atom methods (complexes **10** – **11**) using SHELXS[14] and refined by full–matrix least–squares methods based on F_o^2 with SHELXL–97[14] in the framework of the OLEX2 software.[15] Unless otherwise stated (see ESI), non-hydrogen atoms were refined anisotropically. Coordinates of the hydrogen atoms were calculated in idealized positions and refined as a riding model. In the structures of complexes **1**, **4**, **10**, **11** some atoms were disordered over two places. Alternate positions of involved atoms were refined with site occupation factors constrained to sum to 1.0 and additional SHELXL[14] restraints were applied if necessary; a detailed description of the modelling strategies is provided in the ESI. In all cases, the chemical identity of the compounds was unambiguously determined, the metal coordination environments are well characterized and the chosen final models look acceptable. A summary of the crystallographic and refinement data is reported in Table 1. The supplementary crystallographic data for complexes **1** – **4, 10**, **11** were deposited at the Cambridge Crystallographic Data Center as .cif files, with CCDC numbers 1532872 (**1**), 1532873 (**2**), 1532874 (**3**), 1532875 (**4**), 1532876 (**10**) and 1532877 (**11**). The data can be obtained free of charge via www.ccdc.cam.ac.uk/data_request/cif.

Results and discussion

Synthesis

New six-coordinated rhenium(III) complexes of the general formula [ReX_3(PNPR)] (X = Cl, Br and PNPR = PNPme, PNPet, PNPbu, PNP2, complexes **1** – **9** and **11**) were prepared by reduction/substitution reactions in refluxing ethanol, starting from rhenium(V) precursors ([$Re^{V}OX_3(PPh_3)_2$] (X = Cl, Br) or [NBu_4][$Re^{V}OCl_4$]) and using a precursor/ligand stoichiometric ratio of 1 : 1.5. Variation of the R substituents on the N nitrogen of the diphosphinoamine ligand did not substantially affect the reaction yield; however, the change from chlorine to bromine dramatically reduced the yield of the reaction, and any attempt to improve it, by increasing the amount of the diphosphinoamine ligand and the reaction time or changing the reaction solvents, were unsuccessful. Chloro-complexes **1**, **2**, **4**, **6** and **8** where obtained also by ligand exchange reaction from [$Re^{III}Cl_3$(MeCN)$(PPh_3)_2$], with using a precursor/ligand stoichiometric ratio of 1 : 1 ratio.

Ligand exchange reaction involving the secondary diphosphinoamine ligand (PNPH), as hydrochloride salt (PNPH · HCl), and the [$Re^{III}Cl_3$(MeCN)$(PPh_3)_2$] precursor afforded the complex [$ReCl_3$(PNPH)] (**10**). The hydrochloride salt was neutralized *in situ* by addition of triethylamine in stoichiometric amount. Any attempt to prepare **10** from the respective rhenium(V) precursors failed, as well as any attempt to obtain [$ReBr_3$(PNPH)] by reduction substitution reaction starting from [$Re^{V}OBr_3(PPh_3)_2$]. This may be due to a lower reducing power of this diphosphinoamine in these reaction conditions. Scheme 1 summarizes the reactivity of the PNPR ligands toward precursors.

In all cases, PNPR acts as tridentate ligand generating a six-coordinate complexes characterized by an octahedral geometry (*vide infra*), in which the N of the diphosphinoamine occupies an apical position and the two P atoms lie in the equatorial plane; in this situation, the PNPR can assume *fac* or *mer* configurations. Characterization data (see below) demonstrate that [ReX_3(PNPR)] complexes **1** – **9** were obtained as stable *fac* isomers both in solid and in solution states. In this configuration, the phosphorous atoms are in reciprocal *cis* position, both facing a *trans* halide atom on the octahedral equatorial plane. [$ReBr_3$(PNPme)] (**11**) is an unique exception, since it crystallizes as *mer* isomer, but in solution it seems to prefer the *fac* configuration. In particular, once dissolved in chlorinated solvents, crystalline *mer*-[$ReBr_3$(PNPme)] quantitatively rearranges to the *fac* isomer and, conversely, the formed *fac*-[$ReBr_3$(PNPme)] does not rearrange back to the *mer* form. This behavior was deduced from the ^{1}H NMR spectrum, the voltammetric data (in particular, the value of the potentials of the redox processes, *vide infra*), and the UV/vis spectrum, which are consistent with the spectra and the data of the other *fac*-complexes.

[$ReCl_3$(PNPH)] (**10**) is the only one complex which was found to be stable in the *mer* configuration both in solid and in solution. In this configuration, the two phosphorous and two chloride atoms are mutually in *trans* position.

Obtained data indicate that also in the present case the stereochemistry of this series of rhenium(III)-complexes is determined by the nature of the amino group framed in the diphosphine backbone, clearly resembling the behavior observed in complexes containing the M≡N or the M=NPh metal-nitrogen multiple bonds.[5,6] Thus, the tertiary amine group in PNPR privileges the formation of the kinetically and thermodynamically favored *fac* conformer, whereas the secondary amine function promotes the stabilization of the *mer* isomer as established by the X-ray structure of the complex **10** (see below). Deviation from this behavior was observed for PNPme which yields to both the isomers, when reacted with the [$ReOBr_3(PPh_3)_2$]: the *mer* one is preferred in the crystalline state, whereas the *fac* one is favored in solution.

Table 1 Crystallographic data and structure refinement for the complexes **1 – 4**, **10** and **11**.

	***fac*-[ReCl$_3$(PNPme)] 1**	***fac*-[ReCl$_3$(PNPet)] 2**	***fac*-[ReBr$_3$(PNPet)] 3**	***fac*-[ReCl$_3$(PNPpr)] 4**	***mer*-[ReCl$_3$(PNPH)] 10**	***mer*-[ReBr$_3$(PNPme)] 11**
Empirical formula	$C_{29}H_{31}NP_2Cl_3Re$·DMF	$C_{30}H_{33}NP_2Cl_3Re$	$C_{30}H_{33}NP_2Br_3Re$	$C_{31}H_{35}NP_2Cl_3Re$	$C_{28}H_{29}NP_2Cl_3Re$	$C_{29}H_{31}NP_2Br_3Re$
Formula weight	821.13	762.06	895.44	776.09	734.01	881.42
Temperature/K	302.3(9)	294.4(1)	299.8(4)	297.4(1)	300(3)	298.0(1)
Crystal system	Orthorhombic	Monoclinic	Monoclinic	Monoclinic	monoclinic	orthorhombic
Radiation	MoKα (λ = 0.71073)	MoKα (λ = 0.71073)	MoKα (λ = 0.71073)	MoKα (λ = 0.71073)	MoKα (λ = 0.71073)	MoKα (λ = 0.71073)
Space group	$P\,2_12_12_1$	$P\,2_1/n$	$P\,2_1/n$	$P\,2_1/n$	$I\,2/a$	$Pbca$
***a* / Å**	12.61584(9)	12.3950(3)	12.4502(3)	11.44174(12)	15.9425(3)	17.3668(5)
***b* / Å**	14.38916(10)	18.9802(4)	19.2607(4)	14.86579(11)	14.9601(3)	17.2508(5)
***c* / Å**	18.04782(13)	13.2976(4)	13.4211(3)	19.31565(18)	25.6721(6)	19.9883(6)
***α* / °**	90.00	90.00	90.00	90.00	90.00	90.00
***β* / °**	90.00	112.107(3)	111.117(3)	98.9519(9)	103.822(2)	90.00
***γ* / °**	90.00	90.00	90.00	90.00	90.00	90.00
Volume /Å^3	3276.24(4)	2898.39(12)	3002.25(12)	3245.39(5)	5945.5(2)	5988.3(3)
Z	4	4	4	4	8	8
ρ_{calc} / Mg/m^3	1.665	1.746	1.981	1.588	1.640	1.955
μ / mm^{-1}	4.080	4.601	8.168	4.111	4.483	8.188
***F*(000)**	1632	1504	1720	1536	2880	3376
Crystal size/mm	0.76×0.36×0.16	0.50×0.40×0.20	0.27×0.22×0.18	0.60×0.42×0.28	0.24×0.20×0.11	0.75×0.20×0.15
2ϑ range / °	4.3 to 65.6	4.1 to 57.9	4.1 to 53.0	4.5 to 61.0	4.6 to 59.8	4.7 to 61.5
Reflections collected	68698	38682	33079	60358	46862	61265
Independent reflections/*R*(int)	11414/0.0283	6998/0.0543	5597/0.0315	9337/0.0263	7942/0.0351	8716/0.1284
Data/restraints/parameters	11414/0/402	6998/0/335	5597/0/335	9337/287/344	7942/334/472	8716/142/355
Goodness-of-fit [a] on F^2	1.079	1.053	1.035	1.055	1.077	1.055
Final *R* indexes [$I > 2\sigma(I)$] [b, c]	R_1=0.0181, wR_2=0.0380	R_1=0.0304, wR_2=0.0654	R_1=0.0208, wR_2=0.0456	R_1=0.0225, wR_2=0.0516	R_1=0.0278, wR_2=0.0596	R_1=0.0446, wR_2=0.0993
Flack parameter [16]	-0.018(3)	-	-	-	-	-
Largest diff. peak/hole / e Å^{-3}	0.60/−0.61	1.38/−1.47	0.66/−0.68	0.83/−0.56	1.06/−0.47	2.50/−1.16

[a] Goodness–of–fit = $[\Sigma\,(w\,(F_o^2 - F_c^2)^2] / (N_{obsevns} - N_{params})]^{1/2}$, based on all data; [b] $R_1 = \Sigma\,(\,|F_o| - |F_c|\,) / \Sigma\,|F_o|$; [c] $wR_2 = [\Sigma[w\,(F_o^2 - F_c^2)^2] / \Sigma[w\,(F_o^2)^2]]^{1/2}$.

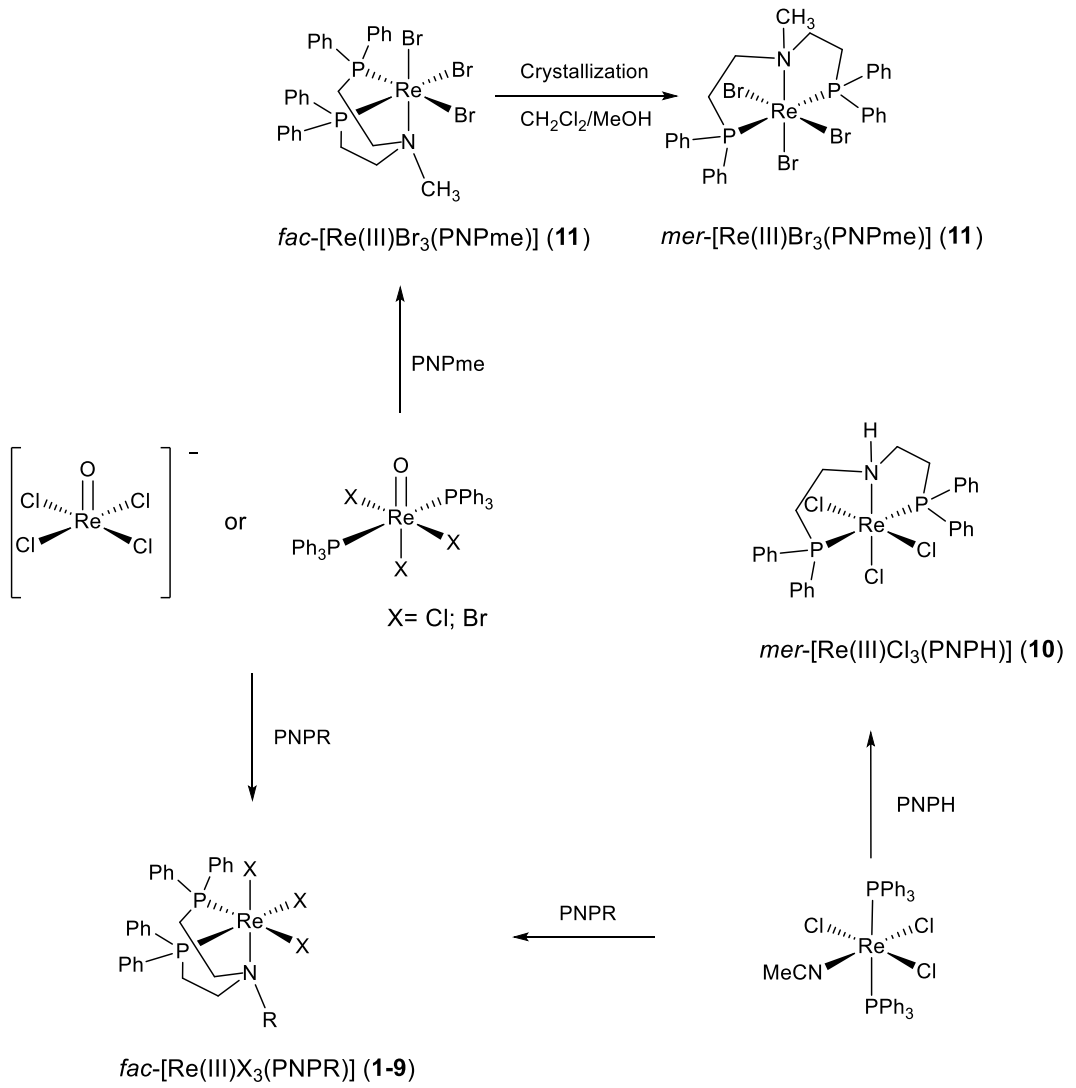

Compound	R	X
1	CH_3	Cl; ---
2; 3	CH_2CH_3	Cl; Br
4; 5	$CH_2CH_2CH_3$	Cl; Br
6; 7	$CH_2CH_2CH_2CH_3$	Cl; Br
8; 9	$CH_2CH_2OCH_3$	Cl; Br

Scheme 1 Reactivity of the PNPR ligands towards different rhenium(V) and rhenium(III) precursors.

Probably, the less-encumbering nature of the methyl group plays a role when the *mer* isomer is selected in the solid state; however, since the analogous chloro-complex was obtained as *fac* isomer both in solution and in solid state, the bromine ligands should also influence this behavior, perhaps disfavoring a facial arrangement of the more bulky halides.

Considering the molecular environments of *fac* versus *mer* compounds, it is reasonable to suppose that the *fac* isomers might be good candidates for further substitution of monodentate halide groups with polydentate ligands, both for steric (a complete face of the octahedron is prone for substitution) and electronic reasons (phosphine P might labilize *trans* positioned halide groups). As proof-of-concept, ligand exchange reactions were performed on **2** and **10** with the selected bis- or tridentate ligands presented in Fig. S1. All attempts to replace the monodentate ligands, in order to mimic the chemistry exhibited by the corresponding [M(N)(PNP)]- and [M(N-Ph)(PNP)]-compounds, failed, indicating that in these $[ReCl_3(PNPR)]$ complexes the halides are chemically inaccessible for this purpose.

Characterization

Elemental analyses are in good agreement with the proposed formulations.

NMR. All the obtained complexes are paramagnetic, as it is typical for octahedral complexes with a low-spin d^4 rhenium(III) center. No signals are displayed in the ^{31}P NMR spectra, consistently with previously reported paramagnetic rhenium(III) complexes.[17] Instead, the ^1H NMR spectra show mostly sharp peaks in a relatively narrow window (about 50 ppm), in which some ^1H-^1H couplings are visible and integrations are consistent (see ESI, Figures S5 – S15). Thus, it was possible to tentatively assign the resonances on the basis of their multiplicities and integrations, as well as through a careful comparison between the spectra. In general, the spectra of the *fac* complexes (**1** – **9** and **11**) show three sets of signals. The first one is assignable to the P*CH₂CH₂*N bridges and comprises four broad singlets or multiplets, each one integrating for two protons, at about: −35.48, −27.33, −3.84 and 7.88 ppm for the chloro-complexes; −33.50, −25.34, −4.21 and 8.16 ppm for the bromo-complexes (mean values; exact chemical shifts are given in Table S1). The second set is represented by the resonances of aromatic hydrogens and includes six signals: two doublets (four protons each) around 14.90 and 11.15 ppm respectively, which are assignable to the *ortho* hydrogens; two triplets (four protons each) around 10.23 and 9.08 ppm respectively, given by the *meta* hydrogens; two triplets (two protons each) around 10.47 and 9.55 ppm respectively, corresponding to the *para* hydrogens. From the observed multiplicities, it looks clear that ^1H-^{31}P and long range ^1H-^1H couplings are absent. Exact chemical shifts are listed in Table S2. The third set of signals is assignable to the R chain, as specified in Table S1. The spectrum of the *mer* complex **10** shows significant differences in the chemical shifts of both the aromatic protons and P*CH₂CH₂*N sets of signals with respect to the *fac* complexes. Notably, the *mer* configuration of **11**, established by the X-ray analysis (*vide infra*), was not confirmed in solution: indeed, the ^1H NMR spectrum shows aromatic protons and P*CH₂CH₂*N sets of signals consistent with those observed in the spectra of the other *fac* complexes, confirming the quantitative conversion of the *mer* isomer to the *fac* one as discussed above.

Cyclic voltammetry. Cyclic voltammetry was performed on all the complexes to explore their redox properties. Data are reported in Table 2 along with cyclic voltammograms of the selected compounds **7** and **8** as representative examples (Fig. 1). All *fac* complexes (**1** – **9** and **11** which in solution is in the *fac* configuration), show a reversible oxidation Re(III)/Re(IV) with potentials in the range 0.185 – 0.005 V. The trend within the chloride series is directly proportional to the inductive effect +I of the N-R substituent: the bigger is the +I effect, the lower is the oxidation potential. The increased electron density at nitrogen makes the complex easier to oxidize. This trend is not observed in the bromide series: likely, the bromine atoms favor the delocalization of the electron density, and contribute to even the +I effect of the different R substituent. Complex **10** does not follow the same course.

In the cathodic region, all the complexes show an intense peak due to the Re(III)/Re(II) reduction, as established by coulometry; this process is irreversible for **1** – **9** and **11** (*fac* complexes), whereas it is reversible for the *mer* complex **10**. Moreover, for **1**, **6**, **8** and all the bromo-complexes, it is clearly visible a reversible couple Re*(III)↔Re*(II) due to the product of a chemical transformation following the Re(III)/Re(II) reduction. Conversely, for **2**, **4** and **11** this reversible couple cannot be seen even at 500 mVs^{-1} scan speed. Within the chloride series, **1** is the easiest to reduce (−1.215 V), whereas **8** is the most stable (−1.48 V), in perfect agreement with the inductive effect. On the contrary, within the bromide series, **9** is the easiest to reduce and **11** the most stable, probably owing to the ability of the bromine atoms to better delocalize the electron density with respect to the chloride analogues.

Table 2 Voltammetric Data for complexes **1** – **11** in dichloromethane[a]

Complex		E°ox Re(III)↔Re(IV) (Volts)	Ered Re(III)→Re(II) (Volts)	Δ(E°ox-Ered) (Volts)	E° Re*(III)↔Re*(II) (Volts)
***mer*-[ReCl₃(PNPH)]**	**10**	0.040	−1.600[b]	1.640	-
***fac*-[ReCl₃(PNPme)]**	**1**	0.185	−1.215	1.400	−0.800
***fac*-[ReCl₃(PNPet)]**	**2**	0.150	−1.460	1.610	-
***fac*-[ReCl₃(PNPpr)]**	**4**	0.140	−1.430	1.570	-
***fac*-[ReCl₃(PNPbu)]**	**6**	0.110	−1.410	1.520	−0.690
***fac*-[ReCl₃(PNP2)]**	**8**	0.005	−1.480	1.485	−0.830
***fac*-[ReBr₃(PNPme)]**	**11**	0.185	−1.380	1.565	-
***fac*-[ReBr₃(PNPet)]**	**3**	0.130	−1.230	1.360	−0.710
***fac*-[ReBr₃(PNPpr)]**	**5**	0.140	−1.250	1.390	−0.660
***fac*-[ReBr₃(PNPbu)]**	**7**	0.140	−1.270	1.410	−0.680
***fac*-[ReBr₃(PNP2)]**	**9**	0.160	−1.120	1.280	−0.760

[a]Data internally referred to the Fc/Fc^+ couple. Data recorded at 200 mVs^{-1}, in dry and degassed dichloromethane with $[n\text{-}Bu_4N][ClO_4]$ (0.1 M) as supporting electrolyte, a platinum-disk working electrode, and a silver-wire quasi-reference electrode. [b]Reversible process.

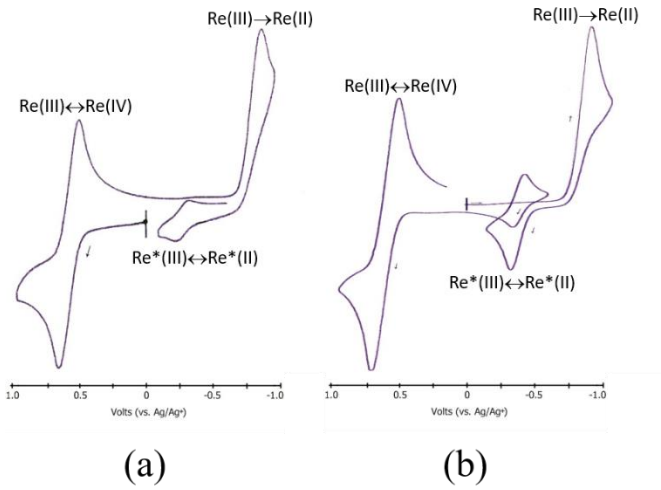

Fig. 1 Cyclic voltammograms of complexes **7** (a) and **8** (b). Data recorded at 200 mVs^{-1}, in dry and degassed dichloromethane with $[n\text{-}Bu_4N][ClO_4]$ (0.1 M) as supporting electrolyte, a platinum-disk working electrode, and a silver-wire quasi-reference electrode. Here, peaks are referred to the Ag/Ag^+ couple. Voltammetric data internally referred to the Fc/Fc^+ couple are given in Table 2.

The latter feature is underlined also by the difference between the anodic and cathodic potentials $\Delta(E°_{ox}\text{-}E_{red})$ of the main redox processes.

Complex **8** is worth of mention, because it is oxidized (E° = +0.005V) and reduced (E = −1.48 V) at the lowest potentials of the *fac*-series. Despite the absence of the corresponding anodic peak and according to the coulometry, this reduction is a one-electron transfer. However, once reduced to Re(II), **8** undergoes a chemical transformation whose product showed a reversible couple at E° = −0.83 V (Fig. 1).

Moreover, it appears that the ether substituent at the nitrogen significantly affects the reduction potential of the complex, probably because of the withdrawing effect of the oxygen, which consistently contributes to shift the reduction potential at the lowest value of the chloride series (E = −1.480 V). Conversely, the reduction potential for the analogous **9** (−1.120 V) is the highest of the bromide series. This indicates that the electron density delocalizing ability of the bromine atoms prevails on the ether-oxygen inductive effect.

As an exception, the *mer* complex **10** show a reversible reduction process, having the highest reduction potential within the series (E° = −1.600 V). Whether this is due to the effect of the different configuration or of the absence of alkyl substituents at the amino nitrogen, is difficult to ascertain.

UV/vis spectroscopy. Electronic spectra of all *fac* chloro-complexes (**1**, **2**, **4**, **6** and **8**, Fig. 2a) show an adsorption maximum at *ca.* 350 nm, whereas for *fac* bromo-complexes **3**, **5**, **7** and **9** an absorbtion band centered at *ca.* 400 nm with a tail extending up to 550 nm is observed (Fig. 2b). Accordingly, the dichlorometane solutions of choloro- and bromo-complexes are nearly colorless and strong yellow colored, respectively. For the unique *mer* chloro-complex (**10**) a red shift to *ca.* 400 nm is observed (indeed, the solution is yellow), along with another absorption band centered at *ca.* 500 nm. **11** shows no significant differences with the other *fac* bromo-complexes, which is

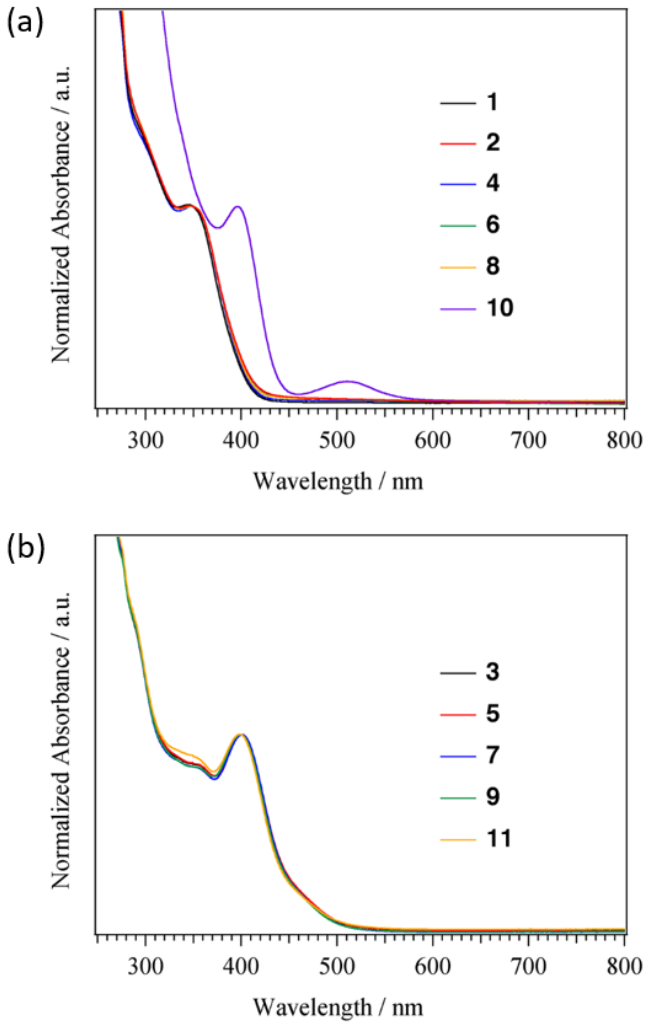

Fig. 2 Normalized electronic spectra of **1**, **2**, **4**, **6**, **8** and **10** (a) and **3**, **5**, **7**, **9**, and **11** (b) in dichlorometane.

another indication that in solution it seems to prefer the facial configuration.

Mass Spectrometry. All complexes were analyzed by electrospray ionization mass spectrometry (ESI-MS). Full spectra of *fac*-$[ReCl_3(PNPR)]$ complexes (Fig. 3b-e) display the protonated molecular ion ($[ReCl_3(PNPR)+H]^+$) and ionic species generated by the consecutive loss of one and two HCl ($[ReCl_3(PNPR)+H–HCl]^+$ and $[ReCl_3(PNPR)+H–2HCl]^+$ respectively). All these fragmentations are confirmed by tandem mass spectra of the single peaks (data not shown). The protonated molecular ion is not present in the spectrum of **10** (Fig. 3a).

A further group of signals might be generated from an oxidation through the insertion of an oxygen atom. The latter species are tentatively assigned to the complexes $[Re^V(O)Cl_3(PNPR)+H]^+$, $[Re^V(O)Cl_3(PNPR)+H–HCl]^+$ and $[Re^V(O)Cl_3(PNPR)+H–2HCl]^+$. Notably, the abundance of such species is inversely proportional to the length of the R group: it reaches its maximum in the spectrum of **1**, while the species are absent in the spectrum of **6**. As an example, collisional experiments on the ion $[Re^V(O)Cl_3(PNPme)+H]^+$ were performed; the spectrum is reported in Fig. S2. Two consecutive HCl losses originates to

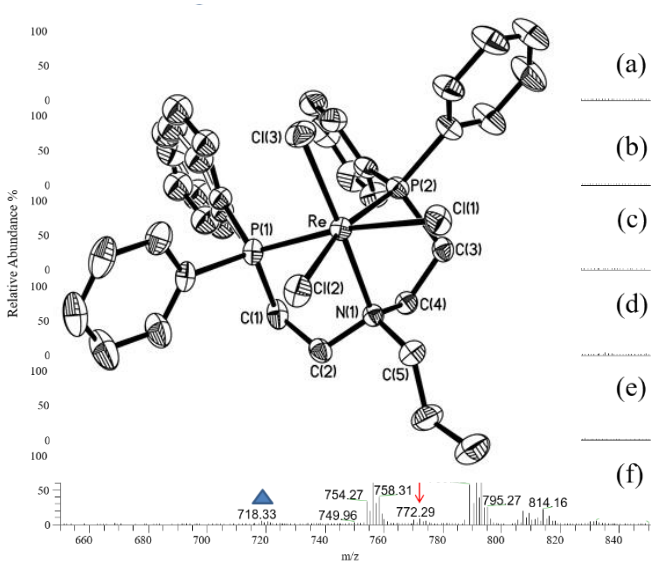

Fig. 3 Partial full scan Full ESI(+)-MS spectra (range: 640 – 850 m/z) of compounds **10** (a), **1** (b), **2** (c), **4** (d), **6** (e) and **8** (f). Red arrows indicates the putative oxo-rhenium(V) ions as discussed in the main text. [★ = $[ReCl_3(PNPR)+H]^+$; ● = $[ReCl_3(PNPR)+H–HCl]^+$; ▲ = $[ReCl_3(PNPR)+H–2HCl]^+$.

the ions $[Re^{V}(O)Cl_3(PNPme)+H–HCl]^+$ (*m/z* 728) and $[Re^{V}(O)Cl(PNPme)+H–2HCl]^+$ (*m/z* 692). A further CO loss is responsible for the ion at *m/z* 664, while the most abundant ions, at *m/z* 499 and 471, can be explained by rearrangement of the PNPR moiety after oxygen loss, with a consequent reduction of the rhenium(V) metal center and might be assigned to the species $[Re^{IV}Cl_2(Ph_2PCH_2CH_2N\text{-}CH_3)]^+$ and $[Re^{III}Cl_2(Ph_2PCH_2CH_3)]^+$, respectively.

fac-$[ReBr_3(PNPR)]$ complexes show similar spectra, with similar fragmentation patterns (Fig. S3). No oxo-species were detected in the ESI-MS spectra of the corresponding *fac*-$[ReBr_3(PNPR)]$ compounds.

The collision of $[ReX_3(PNP2)+H]^+$ ions induces the formation of fragments generated not only by the loss of the two HX, but also by the further cleavage of $–CH_3$ and $–CH_2CH_2OCH_3$ radicals from the alkoxy-alkyl chain of PNP2, as shown in Fig. S4 in the case of $[ReCl_3(PNP2)+H]^+$ ions. This kind of fragmentations at the expense of the alkoxy-alkyl chain were previously observed for other complexes, characterized by the presence of the [Tc(N)(PNP2)]- building block.[18] The fragmentation of the alkyl chain on the N atom was not observed for the other complexes.

X–Ray structure characterization of the complexes 1 – 4, 10 and 11

Details of the crystal structure determinations are listed in Table 1; a selection of bond distances and angles is reported in Table S3. Fig. 4 – 7 report the ORTEP[19] diagrams of the compounds. All the complexes share a distorted octahedral geometry. In *fac* complexes (Table S3), the N(1)–Re–X(3) angle shows a weak tendency to widen, depending on the nature of the alkyl R substituent. The angle grows by 1.2° when R changes from methyl (**1**) to ethyl (**2**) and by an additional 3.1° when R becomes a propyl (**4**); however, the bromide complex **3** fit less well to the trend (+0.3° compared with **1**, but –0.9° compared with **2**). Likewise, the X(1)–Re–X(2) angle opens up by 0.5° when R

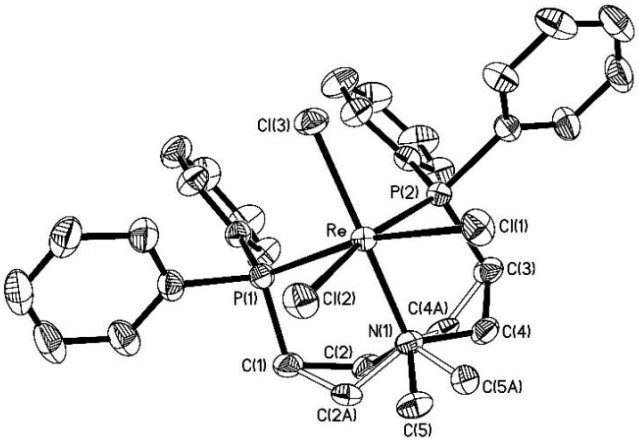

Fig. 6 ORTEP view of complex **4**. Thermal ellipsoids were drawn at the 40% probability level, with hydrogen atoms omitted for clarity. Bonds with alternate positions of atoms in the disordered phenyl ring were drawn in white, with disordered atoms refined only isotropically.

changes from methyl (**1**) to ethyl (**2**) and then by a further 1.3°

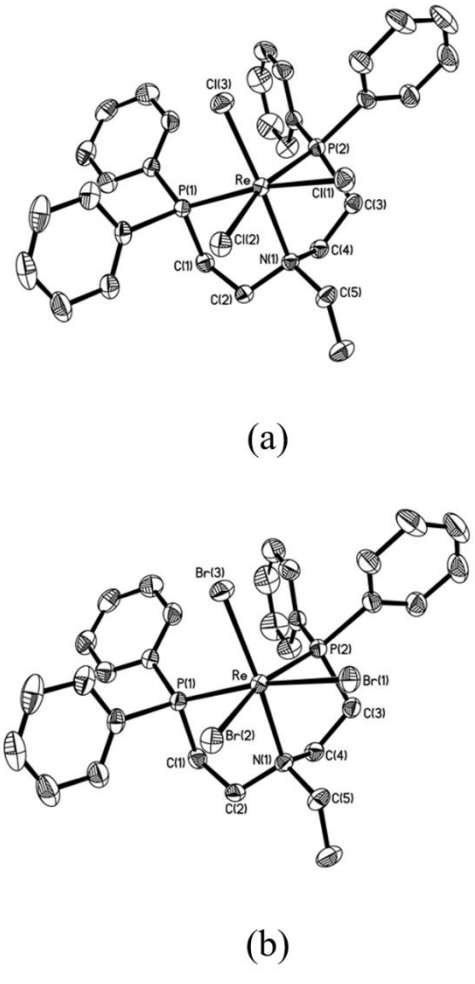

Fig. 5 ORTEP views of complex **2** (a) and **3** (b). Thermal ellipsoids were drawn at the 40% probability level, with hydrogen atoms omitted for clarity.

when R becomes a propyl (**4**), with **3** along the trend. Re–N distances also show a similar behaviour; the bond grows by

about 0.05 Å when R changes from methyl (**1**) to propyl (**4**). Similarly, in *mer* complexes, the Re–N distance grows of *ca.* 0.10 Å passing from 2.156(2) (R = H, **10**) to 2.252(4) Å (R = CH_3, **11**). The mean Re–N distance in *fac* complexes is 2.265 Å (estimated standard deviations for reported mean values not given because of the very limited number of observations involved), 0.06 Å longer than that observed in *mer* complexes, 2.204 Å; complex **1** fits less well to the trend (Re–N distance intermediate between those of **10** and **11**).

The comparison of the average Re–Cl, Re–Br bond lengths indicates that these bonds are longer (+0.02 Å) in *fac* than in *mer* complexes, regardless of the halogen type (2.397 *vs*. 2.373 Å in **1, 2**, **4** and **10**, respectively; 2.538 *vs*. 2.516 Å in **3** and **11**, respectively). These variations do not appear affected by the variation of the R residue.

Mean equatorial Re–X distances in *fac* complexes (for **1**, **2** and **4**, 2.425 Å; for **3**, 2.566 Å) are longer than mean *trans* Re–P bonds (for **1**, **2** and **4**, 2.392 Å; for **3**, 2.409 Å). Hence, Re–X distances look *trans*–labilized by more efficient P donors; a reverse trend looks true for *mer* complexes.

The average Re–Cl, Re–Br bond lengths also reveal a very weak influence of the R residue. In complexes **1**, **2** and **4**, the mean Re–X distances decreases by 0.01 Å when R changes from methyl to propyl, becoming shorter when R becomes heavier. Along with this perspective, our data show that *fac* and *mer* complexes cannot be compared, whereas an attempted comparison between the *mer* complexes **10** and **11**, taking into account the difference in vdW radia of Br (1.85 Å) and Cl (1.75 Å)[20], does not reveal the same trend. All the above comparisons were made in the attempt of spotting any influence due to the R residue. Our data suggest that such influence exist, but it is very faible and involves primarily the N(1) atom, which becomes a little less tightly bound to the metal when the R residue becomes bulkier, besides to the differences due to the *fac* or *mer* arrangement of the halide ligands. This effect is transferred, in an attenuated manner, to the mean Re–X distance, that correspondingly shows a very subtle tendency to shorten when the R residue becomes longer. The donating ability of the tertiary amine nitrogen is then slightly weakened by a growing alkyl residue, allowing a tighter halide–metal bond. Accordingly, a weak variation in the Re–X bonds stability along the series can be expected.

In the CCDC repository[21] we found only a few mononuclear rhenium(III) compounds showing three chloride (or bromide) anions in an X_3P_2N donor set[22a-h]. All the members of this restricted group are *mer* complexes and only one show a bis(diphenylphosphino)ethylamine tridentate ligand similar to those described in this work. Interestingly, there is also another complex showing a similar tridentate ligand, that is bis[(2-di-*t*butylphosphino)ethyl]amine, but in this case the metal is in the +4 oxydation state[22i]. Accordingly, to the best of our knowledge, compounds **1** – **4** are the first reported rhenium(III) *fac* complexes showing the the X_3P_2N donor set provided by an alkylphosphinoethylamine ligand.

Intermolecular contacts are not much represented in complexes **2** – **11**. Instead, the dimethylformamide (DMF) molecule present in the unit cell of **1** substantiates a rather efficient 3D interaction network. A full description of nonbonding interactions in complexes **1**–**11** is given in the ESI (Table S4).

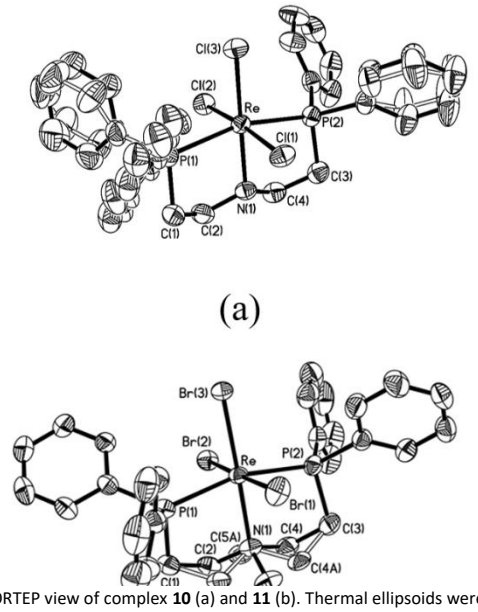

Fig. 7 (a) ORTEP view of complex **10** (a) and **11** (b). Thermal ellipsoids were drawn at the 40% probability level, with hydrogen atoms omitted for clarity. Bonds with alternate positions of disordered atoms in the phenyl rings (a) and in the diphosphinoamine ethylene bridges (b) were drawn in white.

Conclusion

This work is part of our ongoing efforts to explore the coordination chemistry of rhenium along with the prospect of developing metal-based radiopharmaceuticals for nuclear medicine applications. Here we have presented, following previous extensive studies about PNPR complexes of rhenium and technetium in high oxidation states, a further investigation describing rhenium complexes in the +3 oxidation state.

A series of neutral rhenium(III) mixed-ligand complexes, encompassing different PNPR ligands and the Cl^- and Br^- halides have been prepared and fully characterized. As previously observed for the corresponding compounds incorporating the technetium/rhenium nitride or phenylimido cores,[5,6] the stereochemistry of these compounds is determined by the nature of the amino group inserted on the diphosphine backbone as well as by the length of the group chain. Thus, PNPR ligands incorporating a highly nucleophilic tertiary amino group, always stabilize *fac* isomer, except for the less encumbered PNPme donor. In this case, only for *fac*-[$ReBr_3$(PNPme)] complex, a facial to meridional isomerization takes place, when the compound was recrystallized, giving rise to the *mer*-[$ReBr_3$(PNPme)] species. This behavior reproduces that previously found with the PNPme ligand in nitride-Tc(V) complexes[5] (*vide supra*), which gave pacing for embarking this work. Since the analogous chloro-complex **1** assumes instead the *fac* conformation both in solid state and in solution, the bromine ligands likely count in this behavior. Indeed, ligand characterized by the less nucleophilic secondary amino group (PNPH) yield only the stable *mer* form (complex **10**).

Although the *fac* compounds are characterized by molecular properties that in principle may allow the replacement of the three halides with other chelating systems, the complex are inert toward ligand exchange reaction.

Considering the important deferent chemical properties between rhenium and technetium, a possible future extension of this work may be addressed to the translation of this chemistry to the technetium congener.

Acknowledgements

The authors thank the Ministero dell'Istruzione, dell'Università e della Ricerca (MIUR) and the Associazione Italiana per la Ricerca sul Cancro (AIRC) for financial support (MIUR: PON01_2388 and FIRB-MIUR RBAP114AMK_006 RINAME; AIRC: IG 13121). The authors also thank Ms. Anna Moresco for elemental analysis, Dr. Francesco Tisato for his help with NMR, Dr. Gregorio Bottaro for the UV/vis spectroscopy and Dr. Valentina Peruzzo for the mass spectrometry data collection.

Notes and references

1 (a) R. Alberto, in *Technetium, Comprehensive Coordination Chemistry II Volume 5*; ed. J. A. McCleverty, T. J. Meyer, Elsevier, Amsterdam, 2003, 127−270; (b) U. Abram, in *Rhenium, Comprehensive Coordination Chemistry II Volume 5*; ed. J. A. McCleverty, T. J. Meyer, Elsevier, Amsterdam, 2003, 271−402; (c) W. C Eckelman, *JACC Cardiovasc. Imaging*, 2009, **2**, 364.

2 C. Bolzati, D. Carta, N. Salvarese and F. Refosco, *Anti-Cancer Agents Med. Chem.*, 2012, **12**, 428.

3 R. Alberto, H. Braband, D. Can, Y. Tooyama, S. Imstepf, in *Technetium and Other Metals in Chemistry and Medicine*, ed. U. Mazzi, W. C. Eckelman, W. A. Volkert, SGEditoriali, Padova, 2010, 3–12.

4 A. Marchi, L. Marvelli, R. Rossi, L. Magon, L. Uccelli, V. Bertolasi, V. Ferretti and F. Zanobini, *J. Chem. Soc., Dalton Trans.*, 1993, **8**, 1281.

5 (a) C. Bolzati, A. Boschi, L. Uccelli, F. Tisato, F. Refosco, A. Cagnolini, A. Duatti, S. Prakash, G. Bandoli and A. Vittadini, *J. Am. Chem. Soc.*, 2002, **124***,* 11468; (b) A. Boschi, C. Bolzati, E. Benini, E. Malago, L. Uccelli, A. Duatti, A. Piffanelli, F. Refosco and F. Tisato, *Bioconjugate Chem*., 2001, **12**, 1035; (c) C. Bolzati, F. Refosco, A. Cagnolini, F. Tisato, A. Boschi, A. Duatti, L. Uccelli, A. Dolmella, E. Marotta and M. Tubaro, *Eur. J. Inorg. Chem*., 2004, **9**, 1902; (d) F. Tisato, F. Refosco, M. Porchia, C. Bolzati, G. Bandoli, A. Dolmella, A. Duatti, A. Boschi, C. M. Jung, H. J. Pietzsch and W. Kraus, *Inorg. Chem*., 2004, **43**, 8617; (e) A. Boschi, L. Uccelli, C. Bolzati, A. Duatti, N. Sabba, E. Moretti, G. Di Domenico, G. Zavattini, F. Refosco and M. Giganti, *J. Nucl. Med*., 2003, **44**, 806; (f) C. Bolzati, E. Benini, E. Cazzola, C. Jung, F. Tisato, F. Refosco, H. J. Pietzsch, H. Spies, L. Uccelli and A. Duatti, *Bioconjugate Chem*., 2004, **15**, 628; (g) C. Bolzati, A. Mahmood, E. Malago, L. Uccelli, A. Boschi, A. J. Jones, F. Refosco, A. Duatti and F. Tisato, *Bioconjugate Chem*., 2003, **14**, 1231; (h) A. Boschi, L. Uccelli, A. Duatti, C. Bolzati, F. Refosco, F. Tisato, R. Romagnoli, P. G. Baraldi, K. Varani and P. A. Borea, *Bioconjugate Chem*., 2003, **14**, 1279; (i) C. Bolzati, A. Caporale, S. Agostini, D. Carta, M. Cavazza-Ceccato, F. Refosco, F. Tisato, E. Schievano and G. Bandoli, *Nucl. Med. Biol*., 2007, **34**, 511; (j) C. Bolzati, M. Cavazza-Ceccato, S. Agostini, F. Refosco, Y. Yamamichi, S. Tokunaga, D. Carta, N. Salvarese, D. Bernardini and G. Bandoli, *Bioconjugate Chem.*, 2010, **21***,* 928; (k) D. Carta, C. Jentschel, S. Thieme, N. Salvarese, N. Morellato, F. Refosco, P. Ruzza, R. Bergmann, H. J. Pietzsch and C. Bolzati, *Nucl. Med. Biol*., 2014, **41**, 570; (l) S. Thieme, S. Agostini, R. Bergmann, J. Pietzsch, H. J. Pietzsch, D. Carta, N. Salvarese, F. Refosco and C. Bolzati, *Nucl. Med. Biol.*, 2011, **38**, 399.

6 M. Porchia, F. Tisato, F. Refosco, C. Bolzati, M. Cavazza-Ceccato, G. Bandoli and A. Dolmella, *Inorg. Chem.*, 2005, **44**, 4766.

7 (a) G. Bandoli, U. Mazzi, R. Roncari and E. Deutsch, *Coord. Chem. Rev.*, 1982, **44**, 191; (b) F. Tisato, F. Refosco and G. Bandoli, *Coord. Chem. Rev.*, 1994, **135-136**, 325; (c) G. Bandoli, A. Dolmella, M. Porchia, F. Refosco and F. Tisato, *Coord. Chem. Rev.*, 2001, **214**, 43; (d) G. Bandoli, A. Dolmella, F. Tisato and S. Agostini, *Coord. Chem. Rev.*, 2006, **250**, 561; e) H. F. Lang, P. E. Fanwick and R. A. Walton, *Inorg. Chim. Acta*, 2002, **329**, 1; f) Y.-S. Kim, Z. Hea, R. Schibli, S. Liu, *Inorg. Chim. Acta*, 2006, **359**, 2479. g) A. Choualeb, A. J. Lough and D. G. Gusev, *Organometallics*, 2007, **26***,* 3509; h) A. T. Radosevich, J. G. Melnick, S. A. Stoian, D. Bacciu, C. H. Chen, B. M. Foxman, O. V. Ozerov and D. G. Nocera, *Inorg. Chem.*, 2009, **48**, 9214; i) T.L. Nicholson, A. Mahmood, F. Refosco, F. Tisato, P. Müller and A.G. Jones, *Inorg. Chim. Acta*, 2009, **362**, 3637 l) I. Klopsch, M. Finger, C. Würtele, B. Milde, D. B. Werz and S. Schneider, *J. Am. Chem. Soc.*, 2014, **136**, 6881; m) T. J. Korstanje, M. Lutz, J. T. B. H. Jastrzebski and R. J. M. Klein Gebbink, *Organometallics*, 2014, **33**, 2201; n) I. Klopsch, M. Kinauer, M. Finger, C. Würtele and S. Schneider, *Angew. Chem. Int. Ed.*, 2016, **55**, 4786; o) D. Wei, T. Roisnel, C. Darcel, E. Clot and J.-B. Sortais, *ChemCatChem*, 2017, **9**, 80.

8 (a) E. Deutsch, W. Bushong, K. A. Glavan, R. C. Elder, V. J. Sodd, K. L. Scholz, D. L. Fortman and S. J. Lukes, *Science*, 1981, **214**, 85; (b) K. Libson, B. L. Barnett and E. Deutsch, *Inorg. Chem.*, 1983, **22**, 1695; (c) J. L. Vanderheyden, A. R. Ketring, K. Libson, M. J. Heeg, L. Roecker, P. Motz, R. Whittle, R. C. Elder and E. Deutsch, *Inorg. Chem.*, 1984, **23**, 3184; (d) A. Ichimura, W. R. Heineman, J. L. Vanderheyden and E. Deutsch, *Inorg. Chem.*, 1984, **23**, 1272; (e) E. Deutsch, A. R. Ketring, K. Libson, J. L. Vanderheyden and W. Hirth, *Nucl. Med. Biol.*, 1989, **16**, 191; (f) E. Deutsch, *Radiochim. Acta*, 1993, **63**, 195; (g) E. Deutsch, J. L. Vanderheyden, P. Gerundini, K. Libson, W. Hirth, F. Colombo, A. Savi and F. Fazio, *J. Nucl. Med.*, 1987, **28**, 1870; (h) H. J. Pietzsch, H. Spies, P. Leibnitz, G. Reck, J. Berger and R. Jacobi, *Polyhedron*, 1992, **11**, 1623; (i) H. J. Pietzsch, A. Gupta, R. Syhre, P. Leibnitz and H. Spies, *Bioconjugate Chem.*, 2001, **12**, 538; (l) S. Seifert, J. U. Kunstler, E. Schiller, H. J. Pietzsch, B. Pawelke, R. Bergmann and H. Spies, *Bioconjugate Chem.*, 2004, **15**, 856; (m) E. Schiller, S. Seifert, F. Tisato, F. Refosco, W. Kraus, H. Spies and H. J. Pietzsch, *Bioconjugate Chem.*, 2005, **16**, 634.

9 (a) N. Salvarese, N. Morellato, A. Venzo, F. Refosco, A. Dolmella and C. Bolzati, *Inorg. Chem.*, 2013, **52**, 6365; (b) N. Salvarese, A. Dolmella, F. Refosco and C. Bolzati, *Inorg. Chem.*, 2015, **54**, 1634; (c) N. Salvarese, N. Morellato, A. Rosato, L. Meléndez-Alafort, F. Refosco and C. Bolzati, *J. Med. Chem.*, 2014, **57**, 8960.

10 T. L. Nicholson, A. Mahmood, F. Refosco, F. Tisato, P. Müller and A. G. Jones, *Inorg. Chim. Acta*, 2009, **362**, 3637.

11 (a) G. Rouschias and G. Wilkinson, *J. Chem. Soc. A*, 1967, 993; (b) F. A. Cotton and S. J. Lippard, *Inorg. Chem*., 1966, **5**, 9.

12 R. Morassi and L. Sacconi, *J. Chem. Soc. A* 1971, 492.

13 CrysAlisPro, *Agilent Technologies*, Version 1.171.34.47 (release 21-12-2010 CrysAlis171 .NET) for complexes **2** and **4;** Version 1.171.35.19 (release 27-10-2011 CrysAlis171 .NET) for complex **3**; Version 1.171.35.21 (release 20-01-2012 CrysAlis171 .NET) for complex **1**; Version 1.171.36.28 (release 01-02-2013 CrysAlis171 .NET) for complex **6**; Version 1.171.37.35 (release 13-08-2014 CrysAlis171 .NET) for complex **5**.

14 G. M. Sheldrick, *Acta Crystallogr., Sect. A: Found. Adv.*, 2008, **A64**, 112.

15 O. V. Dolomanov, L. J. Bourhis, R. J. Gildea, J. A. K. Howard and H. Puschmann, *J. Appl. Cryst.*, 2009, **42**, 339.
16 H. D. Flack, *Acta Crystallogr., Sect. A: Found. Adv.,* 1983, **A39**, 876.
17 (a) F. A. Cotton and R. L. Luck, *Inorg. Chem*., 1989, **28**, 2181; (b) E. W. Randall and D. Shaw, *J. Chem. Soc. A.*, 1969, 2867; (c) C. Pearson and A. L. Beauchamp, *Inorg. Chim. Acta*, 1995, **237**, 13.
18 M. Tubaro**,** E. Marotta**,** F. Tisato, C. Bolzati, M. Porchia, F. Refosco, P. Tomasin, M. Cavazza-Ceccato and P. Traldi, *Eur. J. Mass Spectrometry*, 2004, **10**, 605.
19 C. K. Johnson, ORTEP, Report ORNL–5138, Oak Ridge National Laboratory, Oak Ridge, TN, 1976.
20 A. Bondi, *J. Phys. Chem*., 1964, **68**, 441.
21 F. H. Allen, *Acta Crystallogr., Sect. B: Struct. Sci., Cryst. Eng. Mater.*, 2002, **B58**, 380; Cambridge Structural Database (Version 5.36 of November 2014 + 3 updates).
22 (a) F. Tisato, F. Refosco, C. Bolzati, A. Cagnolini, S. Gatto and G. Bandoli, *J. Chem. Soc., Dalton Trans.*, 1997, 1421 (CCDC ref. code: RUKPIW); (b) M. Davis, F. Belanger-Gariepy, D. Zargarian, A.L. Beauchamp, *Acta Crystallogr., Sect.C: Cryst. Struct. Commun.*, 1997, **53**, 428 (CCDC ref. code: ANREPS01); (c) V. Bertolasi, A. Marchi, L. Marvelli, R. Rossi, C. Bianchini, I. De los Rios and M. Peruzzini, *Inorg. Chim. Acta*, 2002, **327**, 140 (CCDC ref. code: BAPXIA); (d) H. F. Lang, P. E. Fanwick and R. A. Walton, *Inorg. Chim. Acta*, 2002, **329**, 1 (CCDC ref. code: MOWZAZ); (e) B. Machura, J. O. Dziegielewski and J. Kusz, *Inorg. Chem. Commun.*, 2003, **6**, 786 (CCDC ref. code: HAGTAL); (f) A. R. Cowley, J. R. Dilworth, A. K. Nairn and A.J. Robbie, *Dalton Trans.*, 2005, 680 (CCDC ref. code: FIVKOL); (g) B. Machura, R. Kruszynski and M. Jaworska, *J. Mol. Struct.*, 2005, **740**, 107 (CCDC ref. code: NAMBIN); (h) B. Machura and R. Kruszynski, *J. Mol. Struct.*, 2007, **837**, 92 (CCDC ref. code: KIDVUP).; (i) see ref. 7n (CCDC ref. code: OLEWOT).